THE JOURNAL OF BIOLOGICAL CHEMISTRY
Vol. 279, No. 52, Issue of December 24, pp. 54581–54589, 2004
Printed in U.S.A.

Bcl-2 and Bax Exert Opposing Effects on Ca^{2+} Signaling, Which Do Not Depend on Their Putative Pore-forming Region*

Received for publication, August 23, 2004
Published, JBC Papers in Press, October 12, 2004, DOI 10.1074/jbc.M409663200

Mounia Chami‡§, Andrea Prandini‡, Michelangelo Campanella‡, Paolo Pinton‡, Gyorgy Szabadkai‡¶, John C. Reed‖, and Rosario Rizzuto‡**

From the ‡Department of Experimental and Diagnostic Medicine, Section of General Pathology and the Interdisciplinary Center for the Study of Inflammation, University of Ferrara, 44100 Ferrara, Italy and the ‖Cancer Research Center, The Burnham Institute, La Jolla, California 92037

Recent work has shown that Bcl-2 and other anti-apoptotic proteins partially deplete the endoplasmic reticulum (ER) Ca^{2+} store and that this alteration of Ca^{2+} signaling reduces cellular sensitivity to apoptotic stimuli. We expressed in HeLa cells Bcl-2, Bax, and Bcl-2/Bax chimeras in which the putative pore-forming domains of the two proteins (α5-α6) were mutually swapped, comparing the effects on Ca^{2+} signaling of the two proteins and relating them to defined molecular domains. The results showed that only Bcl-2 reduces ER Ca^{2+} levels and that this effect does not depend on the α5-α6 helices of this oncoprotein. Soon after its expression, Bax increased ER Ca^{2+} loading, with ensuing potentiation of mitochondrial Ca^{2+} responses. Then the cells progressed into an apoptotic phenotype (which included drastic reductions of cytosolic and mitochondrial Ca^{2+} responses and alterations of organelle morphology). These results provide a coherent scenario that highlights a primary role of Ca^{2+} signals in deciphering apoptotic stimuli.

In recent years, great attention has been placed on the possible correlation between the effects of members of the Bcl-2 family of proteins on Ca^{2+} homeostasis and their role in the control of apoptosis (1). Bcl-2 was the first family member proposed to have the ability to alter intracellular Ca^{2+} homeostasis (2). The specific localization of Bcl-2 in the membranes of ER[1] and mitochondria and the demonstration that Bcl-2 acts as an ion channel when inserted into lipid bilayers (3) suggest that Ca^{2+} signaling could be a target of the action of this anti-apoptotic oncoprotein. In previous work, we and others (4, 5) reported that Bcl-2 reduces the state of filling of intracellular Ca^{2+} stores (ER and Golgi apparatus). Consequently, $[Ca^{2+}]$ increases caused by inositol 1,4,5-trisphosphate (IP_3)-generating agonists are blunted in both the cytosol and mitochondria in Bcl-2-overexpressing cells (4, 5). This alteration of intracellular Ca^{2+} homeostasis reduces the efficacy of apoptotic mediators such as ceramide (6). The interference of other members of Bcl-2 family with Ca^{2+} signaling has been described in different models. Lymphocytes from mice lacking Bim do not undergo apoptosis when Ca^{2+} homeostasis is disrupted by ionophores (7). The Bcl-2 homologue Bcl-X_L has been shown to prevent apoptosis of cells at a stage downstream of ER Ca^{2+} release and capacitative Ca^{2+} entry (8). Recently, the pro-apoptotic proteins Bax, Bak, and Bad were also implicated in regulating Ca^{2+} dynamics. Bax/Bak overexpression is reported to favor the transfer of Ca^{2+} from ER to mitochondria, thus inducing cell death (9, 10), and mice deficient in both Bax and Bad show a decrease in ER Ca^{2+} stores and a resistance to a wide range of apoptotic stimuli (11).

Bcl-2 related proteins possess conserved α-helices with sequence conservation clustered in Bcl-2 homology (BH) domains, which enable the different members of the family to form either homo- or heterodimers and to regulate each other (12). Anti-apoptotic members, such as Bcl-2 and Bcl-X_L, harbor at least three BH domains. Among the death promoters, some proteins (*e.g.* Bax, Bak) contain BH1, BH2, and BH3 and closely resemble Bcl-2. Others (*e.g.* Bid, Bad) possess only the BH3 domain. Most Bcl-2-related proteins also contain a C-terminal ~20-residue hydrophobic domain that targets them to intracellular membranes. In the case of Bcl-2, this transmembrane domain functions as a signal anchor that targets and inserts the protein in a N_{cyt}-C_{in} orientation into the two main membrane locations for this protein: the mitochondrial outer membrane and the endoplasmic/nuclear envelope (13). In the case of Bax, the transmembrane domain was reported to permit its translocation from the cytosol to mitochondrial membranes upon overexpression and/or induction of cell death (14). Moreover, recent works have show that Bax is present also in the ER/microsome subcellular compartments (11, 15).

Interestingly, Bcl-2 and related proteins have structural similarities with pore-forming bacterial toxins and can create ion channels in artificial membranes (16, 17). In particular, the predicted fifth and sixth α-helices of Bcl-2 and Bax are hypothesized to directly participate in channel formation. These α-helices are positioned in the core of these proteins and are believed to be inserted into the lipid bilayer with the loop connecting α5 and α6 presumably protruding from the other side of the membrane (16). Indeed, deletion of the α5-α6 regions from Bcl-2 abolishes its ability to form ion channels in synthetic membranes *in vitro* (3). The structural basis for differences in the channels formed *in*

* This work was supported in part by Grants 1285 and GTF02013 from Telethon-Italy, the Italian Association for Cancer Research, the Human Frontier Science Program, the Italian University Ministry (Ministero dell'Università e delle Ricerca Scientifica e Tecnologica and Fondo per gli Investimenti della Ricerca di Base), and the Italian Space Agency (to R. R.). The costs of publication of this article were defrayed in part by the payment of page charges. This article must therefore be hereby marked "*advertisement*" in accordance with 18 U.S.C. Section 1734 solely to indicate this fact.

§ Recipient of an EMBO long term fellowship.

¶ Supported in part by a Marie-Curie individual fellowship (HPMF-CT-2000-00644).

** To whom correspondence should be addressed: Dept. of Experimental and Diagnostic Medicine, General Pathology Section, University of Ferrara, Via L. Borsari 46, 44100 Ferrara, Italy. Tel.: 39-0532-291361; Fax: 39-0532-247278; E-mail: r.rizzuto@unife.it.

[1] The abbreviations used are: ER, endoplasmic reticulum; IP_3, inositol 1,4,5-trisphosphate; AEQ, aequorin probe; SERCA, sarco/endoplasmic reticulum Ca^{2+}-ATPase; Dox, doxycycline; BH, Bcl-2 homology; GFP, green fluorescent protein; BSA, bovine serum albumin; PBS, phosphate-buffered saline.

vitro by Bcl-2 and Bax is unknown but could be due, at least in part, to differences between the polar residues of the α5-α6 regions (reviewed in Ref. 16). In this work, we have employed aequorin-based recombinant probes targeted to specific intracellular localizations and used two cellular models (stable inducible clones *versus* transient expression) to evaluate the effect of Bax overexpression on subcellular Ca^{2+} homeostasis. We then analyzed the role of the presumed channel-forming α5-α6 helices of Bcl-2 and Bax in Ca^{2+} mobilization by using two chimerical constructs in which the putative pore domains of the proteins were mutually swapped.

EXPERIMENTAL PROCEDURES

Reagents—Ionomycin, histamine, ATP, digitonin, *N*-acetyl-D-sphingosine (C_2-ceramide), Geneticin, hygromycin B, and doxycycline were purchased from Sigma-Aldrich, and coelenterazine was purchased from Molecular Probes.

Generation of the Bax Tet-off Cell Line—Bax Tet-off cell lines were generated by co-transfecting pTRE-Bax with pTK-Hyg at a ratio of 20:1, using the calcium phosphate co-precipitation method, into a HeLa Tet-off cell line (HeLa cell line stably transfected with pTet-off regulatory vector with resistance to neomycin) (Clontech, Cambridge, UK). Transfected cells were selected for growth in the presence of 400 μg of hygromycin B and 400 μg of Geneticin/ml of culture medium. Single colonies of resistant cells were tested for doxycycline (Dox) withdrawal-dependent expression of Bax by Western blot.

Cell Culture—HeLa cells and Bax stable clone were grown in Dulbecco's modified Eagles medium supplemented with 2 mM L-glutamine, 100 μg/ml penicillin, 100 μg/ml streptomycin, and 10% fetal calf serum (Cellbio, Euroclone) in 75-cm^2 Falcon flasks. All cells were maintained at 37 °C in 5% CO_2 at 90% relative humidity. The Bax stable clone was maintained in DMEM, 10% fetal calf serum supplemented with hygromycin B and Geneticin in the presence of 2 μg/ml doxycycline (added every 48 h).

Constructs—For calcium analyses, we used aequorin probes targeted to the ER (erAEQ) or mitochondria (mtAEQ-wt and the low affinity probe mtAEQ-mut) or the cytosolic aequorin probe (cytAEQ) (18). For subcellular structural analyses, we used a mitochondrially targeted GFP probe (mtGFP) (18). The wild-type human Bcl-2 and Bax cDNAs and the chimeric Bcl-2/Bax(α5-α6) and Bax/Bcl-2(α5-α6) constructs are cloned in pcDNA3.1 vector (Invitrogen) under the control of the cytomegalovirus promoter (19). The pTRE-Bax construct was generated by subcloning human Bax cDNA into pTRE vector (doxycycline response plasmid) (Clontech) under the control of the tetracycline response element.

Transient Transfection—Transient transfection was carried out using the calcium phosphate co-precipitation method. For aequorin measurements, the cells were seeded onto 13-mm coverslips and co-transfected with the mtGFP (control) or the expression plasmid of interest (Bcl-2, Bax, Bax/Bcl-2(α5-α6), or Bcl-2/Bax(α5-α6) and the various recombinant aequorin probes in a 3:1 ratio (3 μg *versus* 1 μg), thus favoring the expression of the protein of interest in the same subset of cells expressing recombinant aequorin. For mitochondrial morphological analyses and C_2-ceramide experiments, co-transfection was performed on 24-mm glass coverslips with 2 μg of mitochondrial targeted GFP and 6 μg of each construct. Control cells were transfected with 8 μg of mtGFP only. For all experiments analyses were performed 24–36 h after transfection.

Aequorin Measurements—For cytAEQ mtAEQmut and mtAEQwt, 24–36 h post-transfection the coverslips were incubated with 5 μM coelenterazine for 2 h in Krebs-Ringer modified buffer supplemented with 1 mM $CaCl_2$ (KRB: 125 mM NaCl, 5 mM KCl, 1 mM Na_3PO_4, 1 mM $MgSO_4$, 5.5 mM glucose, and 20 mM Hepes, pH 7.4, at 37 °C). For reconstituting erAEQmut with high efficiency the luminal [Ca^{2+}] of the ER was first reduced. This was done by incubating the cells for 1 h at 4 °C in KRB supplemented with 5 μM *n*-coelenterazine, the Ca^{2+} ionophore ionomycin, and 600 μM EGTA. After this incubation, the cells were extensively washed with KRB supplemented with 2% bovine serum albumin (BSA) and 1 mM EGTA before the luminescence measurement was initiated.

All aequorin measurements were carried out in a purpose-built luminometer in KRB supplemented with either 1 mM $CaCl_2$ or 100 μM EGTA. Agonists (ATP or histamine at 100 μM) were added to the same medium (see legends for Figs. 1 and 2). The experiments were terminated by lysing the cells with 100 μM digitonin in a hypotonic Ca^{2+}-rich solution (10 mM $CaCl_2$ in H_2O), thus discharging the remaining aequorin pool. The light signal was collected and calibrated into [Ca^{2+}] values as described previously (18).

Immunofluorescence Analysis—Transfected HeLa cells were fixed in a cold (−20%) methanol:acetone (1:1) solution for 10 min at room temperature and permeabilized with 0.2% Triton X-100 for 10 min. After three washes with PBS, nonspecific binding sites were blocked with 3% BSA for 1 h. Immunostaining was performed with anti-Bax antibody (diluted 1:200 in 3% BSA) for 1 h. After three washes with PBS (5 min each), immunodetection was carried out using Texas Red-conjugated goat anti-rabbit IgG (diluted 1:200 in 3% BSA).

Microscopic Analyses—Mitochondrial morphological analyses were performed 36 h post-transfection. 24-mm coverslips containing the cells were placed in a thermostatted Leyden chamber (model TC-202A; Medical system Corp.) on the stage of a Zeiss Axiovert 200 inverted microscope (Carl Zeiss, SPA, Milano, Italy) equipped with epifluorescence and piezoelectric motorization of the objective (Physik Instrumente). Fluorescent images were captured by a cooled charge-coupled device camera (CoolSnap, Roper Scientific, Inc.) and analyzed using Metamorph 5.0 software (Universal Imaging Corp.). Z-series images were deconvolved using Exhaustive Photon Reassignment (EPR) software, a point spread function-based deconvolution algorithm developed by the University of Massachusetts Imaging Group (20, 21), running on a Linux-based PC.

Apoptosis Analyses—Apoptosis was evaluated by counting apoptotic nuclei (fragmented nuclei) among GFP-positive cells using 7-amino actinomycin D (Sigma-Aldrich) nuclear staining. At 36 h after transfection, cells were fixed with 4% paraformaldehyde in PBS for 20 min. After two washes with PBS, the cells were permeabilized with Triton 0.2% in PBS for 10 min and washed again with PBS. Samples were then incubated with 7-amino actinomycin D at room temperature for 15 min. The percentage of apoptotic cells was calculated from at least 400 GFP-positive cells in three or more independent experiments. For C_2-ceramide treatment, cells transfected with mtGFP alone (control) or co-transfected with mtGFP and the plasmid of interest (see "Transient Transfection") were placed in Dulbecco's modified Eagle's medium supplemented with 2% fetal calf serum and 10 μM C_2-ceramide for 16 h. Cell viability was assessed by microscope count of living GFP-expressing cells. Data are expressed as the percentage of fluorescent cells in different microscope field.

Statistical Analyses—Statistical analyses were performed using Student's *t* test. A p value ≤0.05 was considered significant. All data are reported as means ± S.E.

RESULTS

Transient Overexpression of Bax in HeLa Cells Drastically Reduces Mitochondrial Ca^{2+} Responses but Leaves ER Ca^{2+} Levels Unaffected—The first task of this work was to evaluate the effect of Bax overexpression on subcellular Ca^{2+} homeostasis in transiently transfected HeLa cells, *i.e.* the same cell model in which the effect of Bcl-2 on Ca^{2+} signaling was detected and analyzed previously (4). We used targeted chimeras of the Ca^{2+}-sensitive photoprotein aequorin to monitor the dynamics of agonist-dependent [Ca^{2+}] changes occurring in the cytoplasm and in organelles acting as the source (ER) or target (mitochondria) of Ca^{2+} signals.

We investigated the response to ATP, which acts on G_q-coupled plasma membrane receptors and causes the production of IP_3, thus releasing Ca^{2+} from the ER, followed by sustained influx from the extracellular medium through plasma membrane Ca^{2+} channels. In these experiments, as shown in Fig. 1, HeLa cells were either co-transfected with Bax and the aequorin chimera of interest (*traces* labeled *Bax*) or transfected only with the aequorin probe (controls). Where indicated, the cells were challenged with ATP.

The most striking result was the drastic reduction of the mitochondrial Ca^{2+} rise evoked by agonist stimulation in Bax overexpressing cells: peak value 59 ± 9 μM in Bax cells *versus* 86 ± 9 μM in control cells ($n = 7$, $n = 11$, respectively, $p < 0.01$ (Fig. 1*B*)), *i.e.* a 32% decrease in amplitude *versus* control cells. In contrast, a small (9%), albeit statistically significant reduction was detected in the cytosolic Ca^{2+} peak (peak value 2.1 ± 0.05 μM, $n = 24$ in Bax cells *versus* 2.3 ± 0.06 μM, $n = 38$ in control cells, $p = 0.01$ (Fig. 1*A*)). We then focused our attention on the ER store, given that mitochondria depend on ER Ca^{2+} release for the rapid accumulation of Ca^{2+} in the matrix during

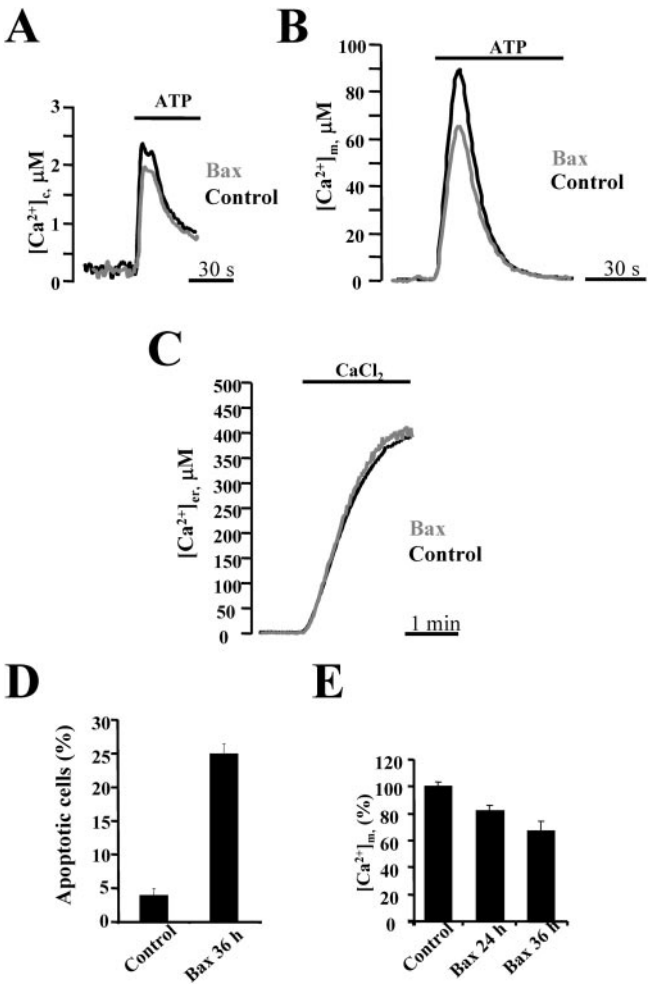

FIG. 1. **Subcellular Ca^{2+} homeostasis in control and Bax transiently expressing HeLa cells.** *A*, cytoplasmic Ca^{2+} homeostasis in control and Bax-transfected cells. $[Ca^{2+}]_c$ measurements were performed in HeLa cells transfected with cytAEQ (*black traces*, control) or co-transfected with cytAEQ and Bax (*gray traces*, Bax). Where indicated, cells were challenged with 100 μM ATP. *B*, mitochondrial Ca^{2+} homeostasis in control and Bax-transfected cells. HeLa cells were either transfected with mtAEQ-mut (*Control*) or co-transfected with mtAEQ-mut and Bax (*Bax*). Where indicated, cells were challenged with 100 μM ATP. *C*, ER Ca^{2+} homeostasis in control and Bax-transfected cells. $[Ca^{2+}]_{ER}$ measurements were performed in HeLa cells transfected with erAEQ (*Control*) or co-transfected with erAEQ and Bax (*Bax*). At 36 h after transfection, the organelles were depleted of Ca^{2+} to optimize aequorin reconstitution (see "Experimental Procedures"). After reconstitution, the cells were transferred to the luminometer chamber and were perfused with KRB/100 μM EGTA. Where indicated, EGTA was replaced with 1 mM $CaCl_2$. These data and those of Figs. 2–6 are representative of at least five independent experiments. *D*, counting of apoptotic bodies (shown as percentage) in HeLa cells transfected with empty pcDNA3.1 vector or transfected with Bax construct was carried out 36 h post-transfection using 7-amino actinomycin D staining. *E*, $[Ca^{2+}]_m$ peak evoked by agonist stimulation in Bax-transfected cells 24 and 36 h post-transfection is represented as a percentage of the peak of control cells.

agonist stimulation (22). In these experiments, in which the Bax cDNA was co-transfected with the erAEQmut aequorin probe, the ER Ca^{2+} store was first depleted of Ca^{2+} during the phase of aequorin reconstitution performed in Ca^{2+}-free medium (as described under "Experimental Procedures"). When Ca^{2+} was added back into the KRB perfusion medium, $[Ca^{2+}]_{ER}$ rose from <10 μM to a plateau value of ~400 μM as reported previously (23, 24). Interestingly, no significant difference was observed between Bax-overexpressing and control cells (410 ± 10 μM, $n = 20$ and 399 ± 9 μM, $n = 31$; $p > 0.1$ (Fig. 1*C*)).

These results showed that Bax *per se* reduces mitochondrial and, to a lesser extent, cytosolic Ca^{2+} signals. Our findings were surprising given that a reduction of ER Ca^{2+} levels and the ensuing reduction of cellular Ca^{2+} signals represent key findings in Bcl-2-overexpressing cells. In agreement with this view (and in apparent contrast with our results), a reduction in ER Ca^{2+} levels and cellular Ca^{2+} signals was detected also in cells in which the Bax/Bak genes were ablated (11). Thus, we considered the possibility that reduction of Ca^{2+} signals is not a direct primary effect of Bax but, rather, that after prolonged high-level expression of Bax, cells have significantly progressed into apoptosis and the down-regulation of Ca^{2+} signaling is part of the final stages of the apoptotic phenotype. In support of this possibility, we observed a high percentage of apoptotic cells in our experimental conditions, *i.e.* cells transiently expressing Bax under the control of a strong cytomegalovirus-derived promoter (Fig. 1*D*). Moreover, we observed that the reduction of mitochondrial agonist-evoked Ca^{2+} signals was proportional to Bax expression. Taking the $[Ca^{2+}]_m$ rise of control cells as 100%, the agonist-evoked $[Ca^{2+}]_m$ peak was reduced in Bax-transfected cells to 82 and 68% at 24 and 36 h post-transfection, respectively (Fig. 1*E*). In this context, to reveal the primary effect of Bax on Ca^{2+} signaling, we proceeded to the generation of a new experimental model in which Bax expression can be finely tuned and its early pro-apoptotic effects can thus be assessed.

Characterization of the Inducible Bax Clone—We generated a cell clone expressing Bax in an inducible manner by stably transfecting a HeLa clonal cell line ($HeLa^{Tet\text{-}off}$) expressing the tetracycline regulatory element with an expression vector in which the Bax cDNA was placed downstream of a tetracycline-repressible promoter. Stable clones were generated by hygromycin selection and screened by Western blotting for conditioned Bax expression. One clone was selected for the following studies that shows a finely tunable up-regulation of Bax expression after induction by doxycycline withdrawal (up to a >2-fold increase after 48 h; see Fig. 2*A*). Bax induction did not alter the protein level of endogenous anti-apoptotic Bcl-2 protein, and thus the rheostat of anti-apoptotic and pro-apoptotic proteins in these cells was modestly affected and depended mainly on the protein level of pro-apoptotic Bax (Fig. 2*A*). Immunostaining analyses revealed the enhancement of the Bax signal, as well as its re-localization to mitochondria upon doxycycline withdrawal (Fig. 2*A*). As a consequence of Bax expression, a modest enhancement of apoptotic cell death was detected 48 h after induction (10% in −Dox cells *versus* 2% in +Dox cells (Fig. 2*B*)), which correlated with a reduction of mitochondrial potential measured by tetramethylrhodamine methyl ester staining intensity (13% reduction in −Dox cells as compared with +Dox cells (Fig. 2*C*)).

Bax Induction Is Associated with a Transient ER Ca^{2+} Overload and an Increase in Mitochondrial Ca^{2+} Signals—We then evaluated ER Ca^{2+} homeostasis in the inducible Bax clone. Twenty-four hours after induction of Bax expression, reconstitution of erAEQmut with coelenterazine was performed in Tet-off cells (as well as in cells maintained under tetracycline gene repression, *i.e.* the controls of this experiment). After transferring the cells to the luminometer chamber, perfusion was initiated with a KRB/EGTA buffer, which was then switched to KRB/Ca^{2+}. In the latter condition, $[Ca^{2+}]_{ER}$ gradually increased, reaching in ~2 min a steady-state plateau value that was markedly different in Bax-induced and control cells. As shown in Fig. 3*A*, Bax induction was associated with an increase of steady-state $[Ca^{2+}]_{ER}$ values (335 ± 13 μM, $n = 17$ in −Dox cells *versus* 255 ± 8 μM, $n = 22$ in +Dox cells, $p \leq 0.0001$) (Fig. 3*A*). Kinetic analysis of IP_3-induced Ca^{2+} release from the

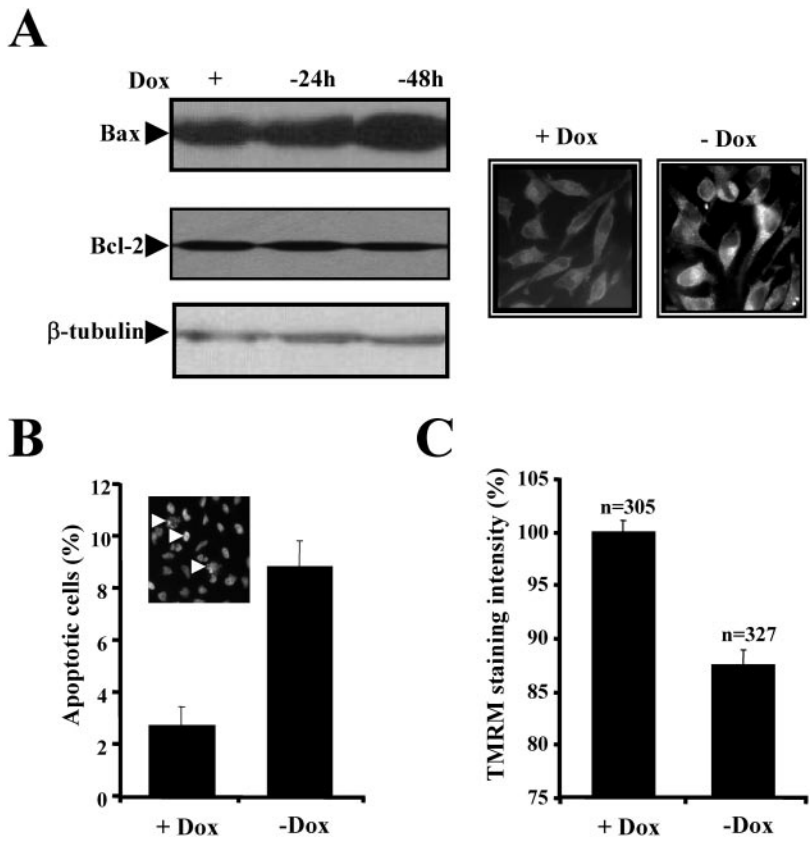

FIG. 2. **Characterization of the Bax-inducible stable clone.** *A*, analysis of Bax expression in stable Bax-expressing clone generated from $HeLa^{Tet\text{-}off}$ cells. Western blot analyses were performed in the presence of doxycycline (+) and 24 or 48 h after doxycycline withdrawal (−24 h and −48 h, respectively). The same blot was successively hybridized with Bax, Bcl-2, and β-tubulin antibodies. Immunolocalization of Bax in Bax/$HeLa^{Tet\text{-}off}$ cells before (+*Dox*) and after (−*Dox*) Bax induction (48 h). *B*, counting of apoptotic bodies (shown as percentage) was performed using DNA dye 7-amino actinomycin D staining in Bax/$HeLa^{Tet\text{-}off}$ cells before and after Bax induction (48 h). Cells with nuclear blebbing considered as apoptotic cells are shown in the *inset*. *C*, mitochondrial tetramethylrhodamine methyl ester (*TMRM*) loading intensity (reflecting mitochondrial potential) in Bax/$HeLa^{Tet\text{-}off}$ cells before and after Bax induction (48 h). *n*, number of cells analyzed.

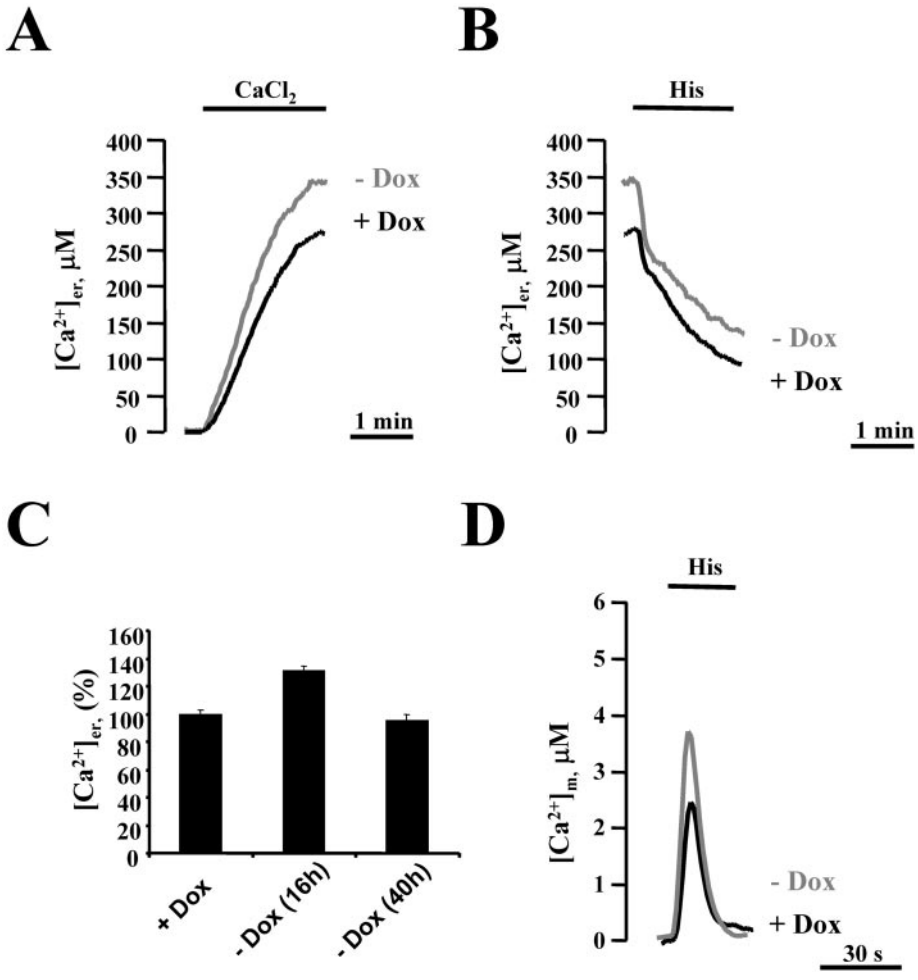

FIG. 3. **Subcellular Ca^{2+} homeostasis in the Bax-inducible clone.** $[Ca^{2+}]$ measurements were performed before (+*Dox*) and 24 h after (−*Dox*) induction. *A*, as in Fig. 1*C*, cells transfected with erAEQ were first perfused with KRB/100 μM EGTA. Where indicated, EGTA was replaced with 1 mM $CaCl_2$ that was maintained until steady-state $[Ca^{2+}]_{ER}$ was reached. *B*, when the steady-state $[Ca^{2+}]_{ER}$ was reached, HeLa cells were stimulated with 100 μM histamine added to KRB/1 mM Ca^{2+}. *C*, $[Ca^{2+}]_{ER}$ in Bax cells (−*Dox*), 24 and 48 h post-induction, is represented as a percentage of the steady state of control cells (+*Dox*). *D*, mitochondrial Ca^{2+} homeostasis. Cells transfected with mtAEQ-wt were perfused with KRB/Ca^{2+} and stimulated with 100 μM histamine where indicated; +Dox and −Dox are represented as *black* and *gray traces*, respectively. All other conditions are as described for Fig. 1.

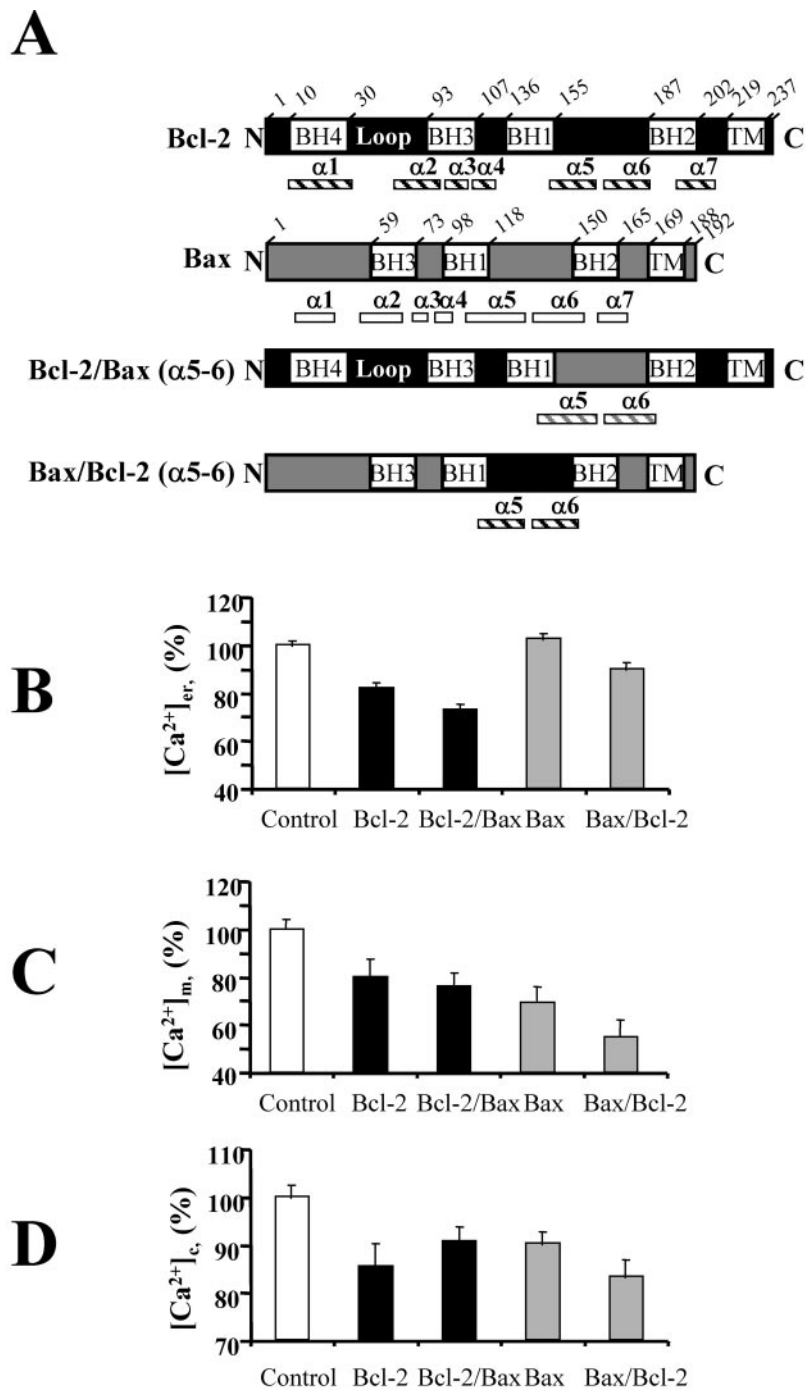

FIG. 4. **Cytosolic, mitochondrial, and ER Ca^{2+} homeostasis in HeLa cells recombinantly expressing Bax, Bcl-2, or Bax-Bcl-2 chimeras.** *A*, schematic representation of the cDNAs employed and the putative regions of the encoded polypeptide. The predicted positions of the α-helical regions within the human Bcl-2 and Bax proteins are shown. Bcl-2/Bax(α5-α6) corresponds to a Bcl-2 construct in which the putative pore-forming domain was replaced with that of Bax. Bax/Bcl-2(α5-α6) corresponds to a Bax construct in which the putative pore-forming domain was replaced with that of Bcl-2 (19). The *numbers* indicate amino acid positions. *BH*, Bcl-2 homology domains; *TM*, transmembrane domain. *B–D*, subcellular Ca^{2+} homeostasis analyses using erAEQmut (*B*), mtAEQ (*C*), and cytAEQ (*D*). $[Ca^{2+}]_{ER}$ steady state (*B*), $[Ca^{2+}]_m$ (*C*), and $[Ca^{2+}]_c$ responses (*D*) evoked by agonist stimulation are represented as percentage of control cells, averaging results from at least five independent experiments ± S.E.

ER revealed a greater initial Ca^{2+} release upon histamine stimulation in Bax-induced cells (Fig. 3*B*). Interestingly, the $[Ca^{2+}]_{ER}$ increase upon Bax induction appeared to be transient; 48 h after the beginning of Bax induction, the $[Ca^{2+}]_{ER}$ value became similar to control cells (240 ± 12 μM, $n = 7$ in −Dox cells) (Fig. 3*C*), thus mimicking the situation of the high-level transient expression of Bax (Fig. 1). We then investigated mitochondrial Ca^{2+} responses. In agreement with the ER data, a larger $[Ca^{2+}]_m$ rise was observed in Bax-induced cells upon histamine stimulation (peak amplitude 4 ± 0.2 μM, $n = 15$ in −Dox cells *versus* 2.5 ± 0.15 μM, $n = 15$ in +Dox cells, $p < 0.01$) (Fig. 3*D*). These results indicate that, as suggested by experiments carried out in other cells models (the Bax/Bak knock-out lines) (11), Bax exerts an opposite effect to Bcl-2 on the state of filling of the ER Ca^{2+} store (increased in the former, reduced in the latter case). In turn, a greater filling of the ER store may allow mitochondrial Ca^{2+} overload and ensuing recruitment of these organelles into apoptotic responses, thus representing an important initiating step in the apoptotic process triggered by this protein.

Establishment of the Role of the Putative Pore-forming Domain (α5-α6) in Ca^{2+} Mobilization by Bax and Bcl-2—An apparent explanation of our results is that the different effects of Bcl-2 and Bax on Ca^{2+} signaling of these proteins are due to differences in the putative pore-forming domain (α5-α6) present in both the pro- and anti-apoptotic family members. To investigate this issue, we used two mutant constructs in which the α5-α6 helices of Bcl-2 and Bax were mutually swapped (Fig. 4*A*) (19) and performed a comparative analysis of subcellular $[Ca^{2+}]$ changes occurring in HeLa cells transiently co-transfected with the appropriate aequorin chimera and either Bcl-2/Bax(α5-α6), Bax/Bcl-2(α5-α6), wild-type Bcl-2, or wild-type

Bax. Ca^{2+} measurements were performed 36 h after transfection, and the results are shown in Fig. 4 as the mean of the $[Ca^{2+}]_{ER}$ steady-state levels (Fig. 4*B*) and of the agonist-evoked Ca^{2+} signals in the mitochondria (Fig. 4*C*) and cytosol (Fig. 4*D*) expressed as a percentage of those of control cells.

These analyses revealed a similar reduction of $[Ca^{2+}]_{ER}$ steady-state levels in Bcl-2/Bax(α5-α6)-transfected (73%) and Bcl-2-transfected cells (80%, Fig. 4*B*). In agreement with this result, in Bcl-2/Bax(α5-α6)- and Bcl-2-transfected cells a comparable reduction was observed in the amplitude of the agonist-dependent $[Ca^{2+}]$ rises of mitochondria (79 and 73% of controls for Bcl-2 and Bcl-2/Bax (α5-α6), respectively (Fig. 4*C*)) and cytosol (85 and 91% of controls for Bcl-2 and Bcl-2/Bax(α5-α6) (Fig. 4*D*)). Conversely, similarly to Bax, overexpression of the Bax/Bcl-2(α5-α6) chimera modestly perturbed ER Ca^{2+} homeostasis (Fig. 4*B*) and greatly reduced the agonist-evoked $[Ca^{2+}]_m$ peak (68 and 54% of controls in Bax and Bax/Bcl-2(α5-α6) (Fig. 4*C*)). The agonist-dependent $[Ca^{2+}]_c$ peak is also slightly diminished (90 and 83% of controls in Bax and Bax/Bcl-2(α5-α6) (Fig. 4*D*)).

Altogether, these data strongly suggest that the putative pore-forming domains of Bcl-2 and Bax are not the key determinants of the different effect of the two proteins on Ca^{2+} homeostasis, as the two chimeric proteins maintain the effect on Ca^{2+} signaling of the native polypeptide and do not acquire that of the introduced α5-α6 helices.

Relationship between Ca^{2+} Dynamics and Apoptotic Regulation by Bcl-2 and Bax Proteins and the Bax/Bcl-2 Chimeras—We reported previously that Bcl-2 prevents mitochondrial damage caused by Ca^{2+} mobilizing apoptotic stimuli, such as ceramide, and protects cells from apoptosis (6). Conversely, Bax was proposed to exert a direct effect on mitochondria to promote apoptosis, with different putative mechanisms: (i) disturbing the mitochondrial membrane barrier function and (ii) binding to the antiapoptotic Bcl-2 family proteins via its BH3 domain, thus inhibiting their function. Mitochondrial Ca^{2+} overload has been shown to promote the opening of the permeability transition pore with ensuing swelling and release of cytochrome *c* and pro-apoptotic factors into the cytosol (25). We previously reported that Ca^{2+} mobilizing apoptotic agents such as C_2-ceramide induce alteration of mitochondrial structure (6). We hypothesized that reduction of mitochondrial Ca^{2+} uptake in Bax and Bax/Bcl-2(α5-α6) mutant overexpressing cells could be the end result of a major morphological alteration of mitochondria structure, which might reduce the sites of close contact between ER and mitochondria and/or the driving force for organelle Ca^{2+} uptake. Thus we investigated whether the expression of Bax, Bcl-2, and the Bax/Bcl-2 chimeras affects mitochondrial structure and/or influences the alterations induced by ceramide, an apoptotic mediator shown to act through mitochondria in a Ca^{2+}-sensitive manner. For this purpose, HeLa cells were transfected with the mitochondrial fluorescent marker mtGFP either alone (controls) or co-transfected with Bcl-2, Bax, or the appropriate Bcl-2/Bax chimera. Then, organelle structure was evaluated at 36 h post-transfection using a digital imaging system (as described in detail under "Experimental Procedures").

First we analyzed Bcl-2 and the Bcl-2/Bax(α5-α6) chimera that shares the property of reducing the Ca^{2+} levels in the ER store with the oncoprotein. Similarly to control cells (Fig. 5*A*), Bcl-2-transfected cells were mostly (85% of analyzed cells) characterized by an interconnected mitochondrial network (Fig. 5*B*). As expected, the Bcl-2/Bax(α5-α6)-transfected cells also showed, in large proportion (69% of analyzed cells), a similar tubular interconnected mitochondrial structure. In all cases, a small percentage of transfected cells with mitochondrial structural rearrangements could be observed (17, 15, and 31% in control, Bcl-2, and Bcl-2/Bax(α5-α6) cells, respectively).

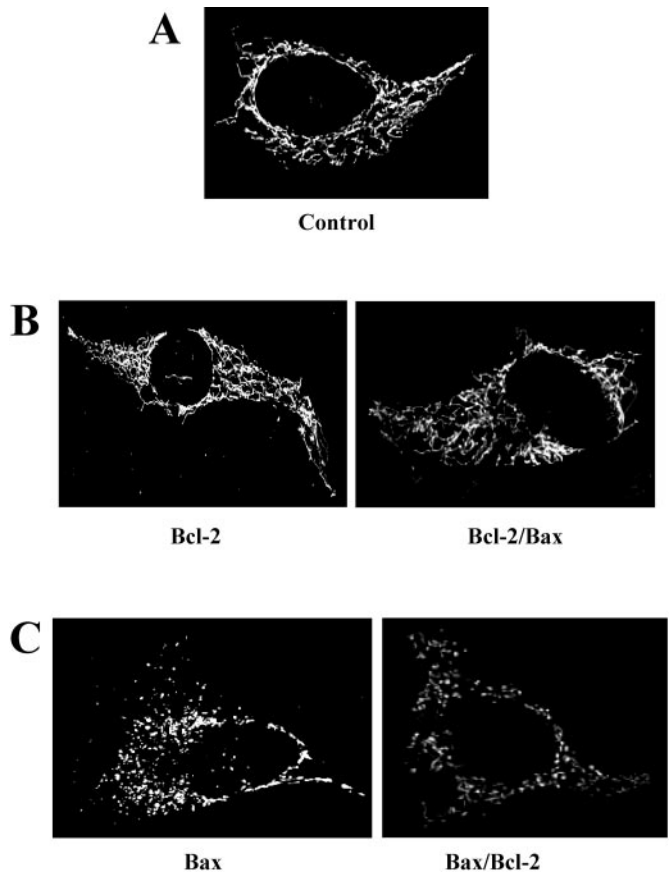

FIG. 5. **Effect of the expression of Bcl-2, Bax, and the Bcl-2/Bax chimeras on mitochondrial morphology.** Analysis of the mitochondrial network structure was performed in HeLa cells transfected with mtGFP (*Control*) or co-transfected with mtGFP and Bax, Bcl-2, or Bcl-2/Bax chimera expression plasmids (see "Experimental Procedures"). The mitochondrial structure was evaluated 36 h post-transfection by visualizing mtGFP with a high resolution digital imaging system. Acquired images were computationally deblurred as described under "Experimental Procedures." *A*, control cells; *B*, Bcl-2- and Bcl-2/Bax(α5-α6)-expressing cells; *C*, Bax- and Bax/Bcl-2(α5-α6)-expressing cells.

We then investigated the effects of Bax and the Bax/Bcl-2(α5-α6) chimera. Fig. 5*C* shows representative images of the mitochondrial network visualized by mtGFP in Bax- and Bax/Bcl-2(α5-α6)-transfected cells. In comparison with control cells (Fig. 5*A*), a major mitochondrial morphological alteration (*i.e.* fragmentation of the network and swelling) was evident in Bax (43% of analyzed cells) and in Bax/Bcl-2(α5-α6) (35% of analyzed cells) overexpressing cells (Fig. 5*A*). The remaining cells were characterized by a partial fragmentation of mitochondria.

The we evaluated the effect of the various chimeras on apoptosis. Firstly, we investigated whether the Bcl-2/Bax(α5-α6) mutant also shared with Bcl-2 the capacity of protecting cells against the apoptotic effect of C_2-ceramide. As reported previously (6), mtGFP was co-transfected with the Bcl-2-related protein of interest, and after C_2-ceramide treatment, the percentage of fluorescent cells was counted. If the protein has no (positive or negative) effect on apoptosis, transfected and non-transfected cells are equally sensitive to the apoptotic agent, and thus albeit the total number of viable cells is reduced, the percentage of transfected cells is the same as in controls. Conversely, the percentage of transfected cells increases if transfected cells are protected (as is the case of anti-apoptotic proteins) and decreases if the protein exerts the opposite effect. As reported previously (6), Bcl-2-transfected cells displayed an

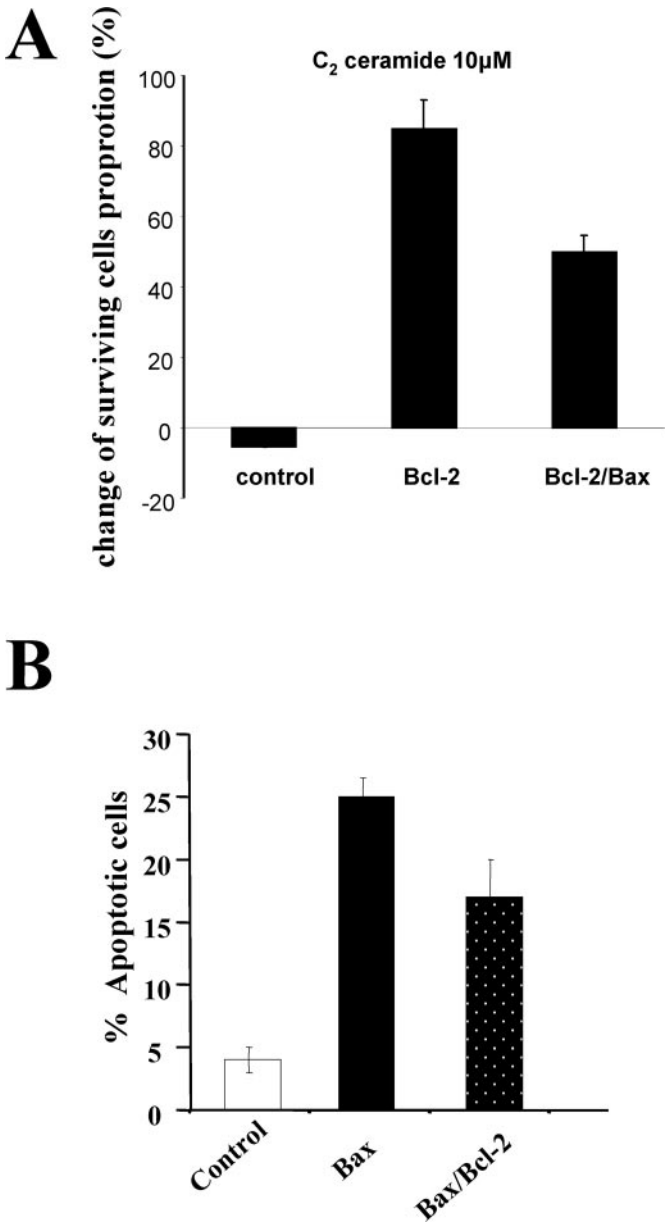

FIG. 6. **Effect on apoptosis of Bcl-2, Bax, and the Bcl-2/Bax chimeras.** *A*, effect of Bcl-2 and Bcl-2/Bax(α5-α6) on C_2-ceramide-induced apoptosis. Cell viability was evaluated after a 16-h treatment with C_2-ceramide (10 μM) in HeLa cells transfected with mtGFP alone (*control*) or co-transfected with mtGFP and Bcl-2- or Bcl-2/Bax-expressing plasmid. The data show the change of percentage of GFP fluorescent cells among the whole cell population (determined by phase contrast microscopy), averaging values obtained by analyzing more than 50 fields in three independent experiments. *B*, effect of Bax and Bax/Bcl-2(α5-α6) on spontaneous apoptosis. Counting of apoptotic bodies (shown as percentage) in HeLa cells transfected with an empty pcDNA3.1 vector (control) or transfected with Bax or with Bax/Bcl-2 constructs was determined 36 h post-transfection using 7-amino actinomycin D staining.

enhanced survival and thus a protective effect against C_2-ceramide treatment (Fig. 6*A*). No change in the percentage of living fluorescent cells was noted in control cells transfected with mtGFP alone (22% ± 1 in C_2-ceramide-treated control cells *versus* 20 ± 3% in nontreated control cells). Interestingly, the Bcl-2/Bax(α5-α6) mutant also conferred a protective effect against C_2-ceramide (Fig. 6*A*). Thus both wild-type Bcl-2 and the Bcl-2/Bax(α5-α6) chimera protect against ceramide-induced apoptosis, combining that with their effects on ER Ca^{2+} homeostasis.

Finally, we evaluated the capacity of Bax and the Bax/Bcl-2(α5-α6) chimera to induce spontaneous apoptosis (Fig. 6*B*). In agreement with their similar effects on Ca^{2+} signaling (see Fig. 4) and on mitochondrial structure (see Fig. 5*B*), wild-type Bax and the Bax chimera with the Bcl-2 α5-α6 helices show a very similar capacity to induce apoptosis. Indeed, upon Bax and Bax/Bcl-2(α5-α6) expression, 25 ± 4% and 19 ± 5% of cells, respectively, showed morphological signs of spontaneous apoptosis, without the exogenous addition of apoptotic stimuli (Fig. 6*B*).

DISCUSSION

The link between dysregulation of calcium homeostasis and the control of apoptosis has been strengthened by a series of experimental observations converging into a coherent scheme. The most thoroughly investigated case is that of Bcl-2. The first evidence was obtained in cell clones stably expressing the oncoprotein, and it indicated that Bcl-2 maintains ER Ca^{2+} filling and prevents the unloading of ER Ca^{2+} content caused by various pro-apoptotic conditions (*e.g.* treatment with the SERCA pump inhibitor, thapsigargin (26)). However, more recently, experiments with different probes and cell models demonstrated a reduction of ER Ca^{2+} level upon Bcl-2 expression (5, 27) and, conversely, a reduction when Bcl-2 endogenous expression was silenced (11). The partial emptying of agonist-sensitive Ca^{2+} stores and the ensuing reduction of cellular Ca^{2+} responses have been shown to be part of the protecting mechanism against apoptotic stimuli such as ceramide (6) and hydrogen peroxide or arachidonic acid (11). The investigation of pro- and anti-apoptotic proteins of viral origin then showed that the manipulation of Ca^{2+} signaling is not restricted to this important oncogene but may represent a more general mechanism in the control of apoptosis. Indeed, the anti-apoptotic Coxsackie viral protein 2B has been shown to reduce ER Ca^{2+} levels (28). Interestingly, the pro-apoptotic protein X of hepatitis B (HBX) has been shown to enhance cellular responses to agonists not by altering ER Ca^{2+} levels but by inducing the caspase-dependent cleavage of the plasma membrane Ca^{2+} pump (29). In this scenario, it is expected that the pro-apoptotic members of the Bcl-2 family do not share with Bcl-2 itself the capacity of reducing ER Ca^{2+} levels or may even have the opposite function. Evidence that the latter is most likely the case was provided by Scorrano *et al*. (11) who have shown that gene ablation of Bax and Bak causes a reduction of ER Ca^{2+} levels and ensuing resistance to Ca^{2+}-dependent apoptotic stimuli, similar to what has been reported for Bcl-2 overexpression.

The effect of Bax on intracellular Ca^{2+} homeostasis was directly addressed in this paper, investigating (i) whether recombinant expression of Bax affected the ER Ca^{2+} levels and agonist-dependent responses of the cells and (ii) the structural basis for the different actions of Bcl-2 and Bax. Two expression systems were employed: (i) transient expression under the control of a constitutive promoter and (ii) a stable clone in which conditional expression of Bax was driven by a tetracycline-regulated promoter, and thus levels and timing of the expression could be more finely tuned. The combination of the two series of data provided significant information regarding the time course and dose dependence of the effect of Bax overproduction. The primary effect of Bax on Ca^{2+} homeostasis was evident in the conditional expression system, relatively soon after the induction of low level Bax expression. At this phase, still no significant increase in the number of apoptotic cells was detected, and thus the detected changes in Ca^{2+} homeostasis were not due to late secondary apoptotic alterations. Under these conditions, we observed an increase in ER Ca^{2+} levels

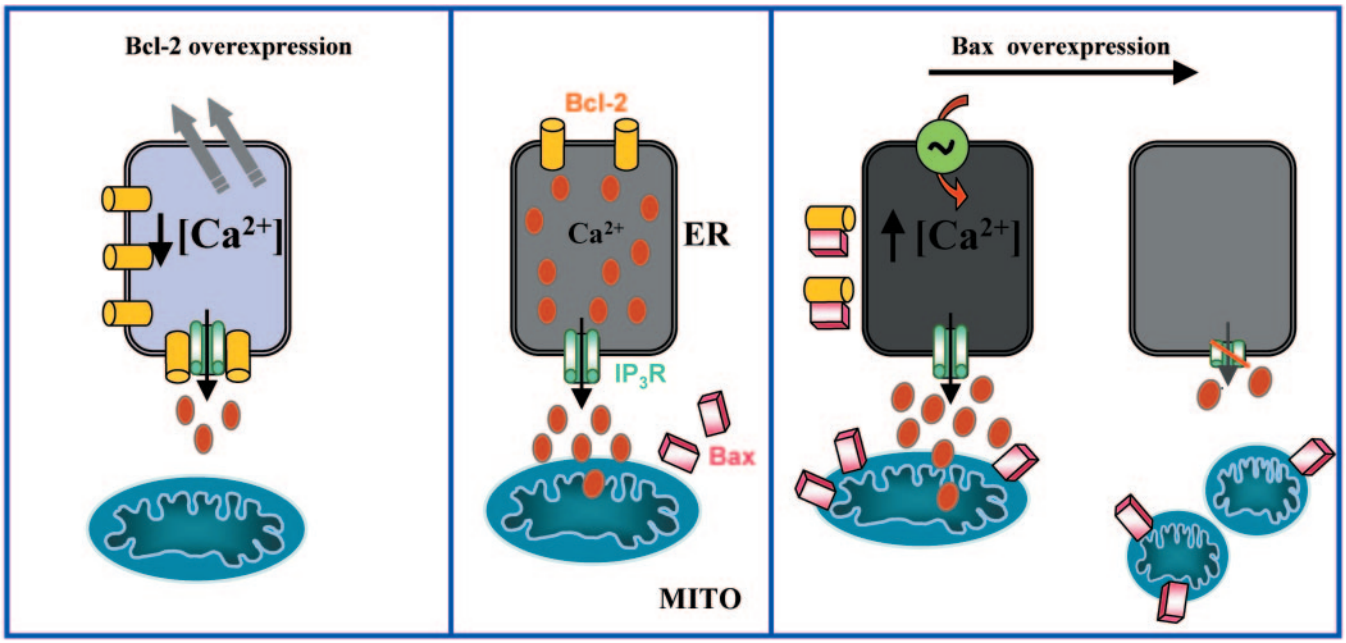

FIG. 7. **Schematic model of Bcl-2 and Bax effects on Ca^{2+} homeostasis.** Bax and Bcl-2 both modify intracellular Ca^{2+} homeostasis independently of their putative pore-forming domain (α5-α6). Bcl-2 reduces ER Ca^{2+} levels (and protects from apoptotic stimuli acting through Ca^{2+} release from the ER), whereas Bax initially enhances the loading of the ER Ca^{2+} store leading to mitochondrial Ca^{2+} overload and morphological alterations and ultimately impairs ER Ca^{2+} release upon cell stimulation, reducing both cytosolic and mitochondrial Ca^{2+} signals. *IP_3R*, IP_3 receptor; *MITO*, mitochondria.

that correlated with an increase in mitochondrial Ca^{2+} loading upon challenging of cells with stimuli, causing the release of Ca^{2+} from the ER Ca^{2+} pool. These results agree with findings from Bax/Bak knock-outs (11). Furthermore, this observation is in agreement with the work by Snyder and co-workers (30) who demonstrated that the initial release of cytochrome *c* potentiates IP_3-mediated Ca^{2+} release, forming a positive feedback loop to activate the mitochondrial phase of apoptosis. Conversely, when Bax was transiently expressed attaining high protein level, as well as when Bax expression was prolonged in the inducible clone, no difference became detectable between the steady-state $[Ca^{2+}]_{ER}$ levels of controls and Bax-expressing cells. Under those conditions, two features dominated the general picture of Ca^{2+} signaling. The first was a drastic perturbation of mitochondrial three-dimensional structure and of key functional parameters, including mitochondrial membrane potential and the Ca^{2+} uptake capacity of the organelle. This effect also provides a possible explanation for the gradual decrease in ER Ca^{2+} loading; reduced ATP provision to the SERCA pumps could gradually impair Ca^{2+} (re)accumulation into the ER, thus bringing the $[Ca^{2+}]_{ER}$ steady-state levels to those of a control cell. An alternative possibility can be presumed from the recent demonstration that the IP_3 receptor includes a consensus site for caspase-3 cleavage, and the cleaved form of the receptor exhibits increased leakiness and reduced sensitivity to IP_3 (31, 32). The latter finding would account not only for the reduction of steady-state $[Ca^{2+}]_{ER}$ but also for the second obvious feature of the late apoptotic phenotype, *i.e.* the reduction of the Ca^{2+} release rate from the ER upon cell stimulation. In turn a smaller Ca^{2+} release results in the reduction of the amplitude of cytosolic Ca^{2+} responses (an effect that cooperates with the direct effect on mitochondria in causing the dramatic 30–50% reduction of mitochondrial $[Ca^{2+}]$ peaks).

We then investigated whether the different effect on ER Ca^{2+} homeostasis of Bcl-2 and Bax depended on the properties of the putative pore-forming region. For this purpose, we employed two chimeras generated by us, in which the α-helices that were proposed to form the ion channel of Bcl-2(α5-α6) were mutually swapped between the two proteins (19). The prediction was that if the putative pore-forming region is the determinant of the effect on Ca^{2+} signaling, the α5-α6 helices would transfer this modulatory effect from the protein from which it is derived to the protein in which it is inserted. Thus, in transient expression experiments, one would predict that a Bcl-2 protein with the α5-α6 helices of Bax should induce no alteration of ER Ca^{2+} levels (as observed with Bax itself), whereas a Bax protein with the α5-α6 helices of Bcl-2 should partially empty the ER store. This was clearly not the case; the insertion of the α5-α6 helices of the other protein did not modify the primary effect on Ca^{2+} signaling of Bax and Bcl-2, implying that this effect does not depend on their putative pore-forming domain. Similarly, the two chimeras retained the effects on apoptosis of the original protein: the Bax protein with Bcl-2(α5-α6) helices is pro-apoptotic and causes perturbation of mitochondrial structure and function (including the drastic reduction of $[Ca^{2+}]_m$ responses), whereas the Bcl-2 chimera with Bax(α5-α6) protects against stimuli, such as ceramide, acting through a calcium and mitochondria-dependent pathway. Thus, one should conclude that (i) either the alteration of Ca^{2+} signaling is not due to the channel activity of these regions but depends on the modulation of the activity of other resident channels, or (ii) if an intrinsic channel activity is responsible for the effect, a different regulation occurs in the two proteins. In all cases, the key determinant of the signaling specificity rests in a part of the molecules that is distinct from their putative pore-forming domain (the α5-α6 helices). Similar conclusions were drawn from two recent works regarding the structure/function relationship of Bax and Bcl-2. Namely, Bax(α5-α6) was shown to be essential for Bax-mediated cytochrome *c* release (33), but the modulation of the adenine nucleotide translocase, taking part in the mitochondrial permeability transition pore, presumably requires interaction of other parts of the Bax and Bcl-2 proteins (34). Moreover, in linking Bcl-2 to cellular Ca^{2+} signaling through a mechanism independent of the pore-forming domain, our results are sup-

ported by the finding of Bassik *et al*. (35), who showed that the ability of Bcl-2 to lower $[Ca^{2+}]_{ER}$ and to protect against Ca^{2+}-dependent death stimuli depends on a regulatory event, *i.e.* on the stimulation of IP_3 receptor phosphorylation, leading to the consequent increase of the leakiness of the ER resident Ca^{2+} channel.

The general picture emerging from these results (Fig. 7) is that Bax and Bcl-2 both have an effect on Ca^{2+} signaling that does not depend on the region proposed to form an ion channel but resides in a yet unidentified segment of the proteins. Moreover, it is unclear from these studies whether the ability of Bcl-2 and Bax to regulate ER $[Ca^{2+}]$ is an intrinsic property of these proteins *versus* a manifestation of a regulatory effect on other proteins. As reported previously, Bcl-2 reduces ER Ca^{2+} levels, and consequently it moderates the efficacy of apoptotic mediators that use Ca^{2+} signals (and the involvement of mitochondria as downstream effectors) as a potentiation/commitment factor. Conversely, Bax enhances the loading of the ER Ca^{2+} store and thus boosts the Ca^{2+} load to which the apoptotic effector systems (including mitochondria) are exposed upon physiological and/or pathological challenges. This effect of Bax coincides with gross perturbation of mitochondrial structure and function and finally, later in apoptotic progression, to the development of an altered signaling phenotype, which includes impaired ER Ca^{2+} release upon cell stimulation and thus reduction of cellular Ca^{2+} signals. Although much remains to be understood about the molecular targets of these signaling alterations, these results strongly reaffirm the notion of the involvement of Ca^{2+} in the control of apoptosis and suggest possible opportunities for developing pharmacological modulators of this pathophysiological event.

REFERENCES

1. Demaurex, N., and Distelhorst, C. (2003) *Science* **300,** 65–67
2. Baffy, G., Miyashita, T., Williamson, J. R., and Reed, J. C. (1993) *J. Biol. Chem.* **268,** 6511–6519
3. Schendel, S. L., Xie, Z., Montal, M. O., Matsuyama, S., Montal, M., and Reed, J. C. (1997) *Proc. Natl. Acad. Sci. U. S. A.* **94,** 5113–5118
4. Pinton, P., Ferrari, D., Magalhaes, P., Schulze-Osthoff, K., Di Virgilio, F., Pozzan, T., and Rizzuto, R. (2000) *J. Cell Biol.* **148,** 857–862
5. Foyouzi-Youssefi, R., Arnaudeau, S., Borner, C., Kelley, W. L., Tschopp, J., Lew, D. P., Demaurex, N., and Krause, K. H. (2000) *Proc. Natl. Acad. Sci. U. S. A.* **97,** 5723–5728
6. Pinton, P., Ferrari, D., Rapizzi, E., Di Virgilio, F. D., Pozzan, T., and Rizzuto, R. (2001) *EMBO J.* **20,** 2690–2701
7. Bouillet, P., Metcalf, D., Huang, D. C., Tarlinton, D. M., Kay, T. W., Kontgen, F., Adams, J. M., and Strasser, A. (1999) *Science* **286,** 1735–1738
8. Pan, Z., Damron, D., Nieminen, A. L., Bhat, M. B., and Ma, J. (2000) *J. Biol. Chem.* **275,** 19978–19984
9. Nutt, L. K., Pataer, A., Pahler, J., Fang, B., Roth, J., McConkey, D. J., and Swisher, S. G. (2002) *J. Biol. Chem.* **277,** 9219–9225
10. Nutt, L. K., Chandra, J., Pataer, A., Fang, B., Roth, J. A., Swisher, S. G., O'Neil, R. G., and McConkey, D. J. (2002) *J. Biol. Chem.* **277,** 20301–20308
11. Scorrano, L., Oakes, S. A., Opferman, J. T., Cheng, E. H., Sorcinelli, M. D., Pozzan, T., and Korsmeyer, S. J. (2003) *Science* **300,** 135–139
12. Gross, A., McDonnell, J. M., and Korsmeyer, S. J. (1999) *Genes Dev.* **13,** 1899–1911
13. Krajewski, S., Tanaka, S., Takayama, S., Schibler, M. J., Fenton, W., and Reed, J. C. (1993) *Cancer Res.* **53,** 4701–4714
14. Goping, I. S., Gross, A., Lavoie, J. N., Nguyen, M., Jemmerson, R., Roth, K., Korsmeyer, S. J., and Shore, G. C. (1998) *J. Cell Biol.* **143,** 207–215
15. Krajewski, S., Blomqvist, C., Franssila, K., Krajewska, M., Wasenius, V. M., Niskanen, E., Nordling, S., and Reed, J. C. (1995) *Cancer Res.* **55,** 4471–4478
16. Schendel, S. L., Montal, M., and Reed, J. C. (1998) *Cell Death Differ.* **5,** 372–380
17. Saito, M., Korsmeyer, S. J., and Schlesinger, P. H. (2000) *Nat. Cell Biol.* **2,** 553–555
18. Chiesa, A., Rapizzi, E., Tosello, V., Pinton, P., de Virgilio, M., Fogarty, K. E., and Rizzuto, R. (2001) *Biochem. J.* **355,** 1–12
19. Matsuyama, S., Schendel, S. L., Xie, Z., and Reed, J. C. (1998) *J. Biol. Chem.* **273,** 30995–31001
20. Carrington, W. A., Lynch, R. M., Moore, E. D., Isenberg, G., Fogarty, K. E., and Fay, F. S. (1995) *Science* **268,** 1483–1487
21. Rizzuto, R., Carrington, W., and Tuft, R. A. (1998) *Trends Cell Biol.* **8,** 288–292
22. Rizzuto, R., Brini, M., Murgia, M., and Pozzan, T. (1993) *Science* **262,** 744–747
23. Barrero, M. J., Montero, M., and Alvarez, J. (1997) *J. Biol. Chem.* **272,** 27694–27699
24. Pinton, P., Pozzan, T., and Rizzuto, R. (1998) *EMBO J.* **17,** 5298–5308
25. Green, D. R., and Kroemer, G. (2004) *Science* **305,** 626–629
26. Lam, M., Dubyak, G., Chen, L., Nunez, G., Miesfeld, R. L., and Distelhorst, C. W. (1994) *Proc. Natl. Acad. Sci. U. S. A.* **91,** 6569–6573
27. Rizzuto, R., Pinton, P., Ferrari, D., Chami, M., Szabadkai, G., Magalhaes, P. J., Di Virgilio, F., and Pozzan, T. (2003) *Oncogene* **22,** 8619–8627
28. Campanella, M., de Jong, A. S., Lanke, K. W., Melchers, W. J., Willems, P. H., Pinton, P., Rizzuto, R., and van Kuppeveld, F. J. (2004) *J. Biol. Chem.* **279,** 18440–18450
29. Chami, M., Ferrari, D., Nicotera, P., Paterlini-Brechot, P., and Rizzuto, R. (2003) *J. Biol. Chem.* **278,** 31745–31755
30. Boehning, D., Patterson, R. L., Sedaghat, L., Glebova, N. O., Kurosaki, T., and Snyder, S. H. (2003) *Nat. Cell Biol.* **5,** 1051–1061
31. Assefa, Z., Bultynck, G., Szlufcik, K., Kasri, N. N., Vermassen, E., Goris, J., Missiaen, L., Callewaert, G., Parys, J. B., and De Smedt, H. (2004) *J. Biol. Chem.* **279,** 43227–43236
32. Nakayama, T., Hattori, M., Uchida, K., Nakamura, T., Tateishi, Y., Bannai, H., Iwai, M., Michikawa, T., Inoue, T., and Mikoshiba, K. (2004) *Biochem. J.* **377,** 299–307
33. Heimlich, G., McKinnon, A. D., Bernardo, K., Brdiczka, D., Reed, J. C., Kain, R., Kronke, M., and Jurgensmeier, J. M. (2004) *Biochem. J.* **378,** 247–255
34. Brenner, C., Cadiou, H., Vieira, H. L., Zamzami, N., Marzo, I., Xie, Z., Leber, B., Andrews, D., Duclohier, H., Reed, J. C., and Kroemer, G. (2000) *Oncogene* **19,** 329–336
35. Bassik, M. C., Scorrano, L., Oakes, S. A., Pozzan, T., and Korsmeyer, S. J. (2004) *EMBO J.* **23,** 1207–1216